

# Free Vibrations of a Thin-Walled Cylindrical Shell Subjected to a Bending Moment

V. I. WEINGARTEN\*

University of Southern California, Los Angeles, Calif.

The effect of a bending moment on the free vibrations of a thin-walled cylindrical shell is investigated by means of a modified Donnell equation. An experimental investigation was performed in conjunction with the analysis. The results indicate that, as the bending moment increases, some frequencies increase in magnitude while others decrease which is contrary to results obtained for symmetric loadings.

## Nomenclature

$a_n$	= coefficients in deflection function
$D$	= flexural stiffness of cylinder wall, $[Eh^3/12(1 - \nu^2)]$ , lb-in.
$E$	= Young's modulus of cylinder material, psi
$f$	= frequency $[f = (\omega/(2\pi))]$ , cps
$g$	= gravitational acceleration, in./sec <sup>2</sup>
$h$	= thickness of cylinder, in.
$L$	= length of cylinder, in.
$m - 1$	= number of nodes in axial mode shape
$M$	= applied bending moment, in.-lb
$n$	= number of circumferential waves in mode shape for $M = 0$
$p$	= external pressure, positive inward, psi
$p^*$	= pressure parameter $\{p/E(R/h)^2[12(1 - \nu^2)]^{1/2}\}$
$P$	= applied compressive load, lb
$q$	= surface loading, psi
$R$	= radius of cylinder, in.
$r, s$	= integers
$S$	= radius-thickness parameter $\{[12(1 - \nu^2)]^{1/2}(R/h)\}$
$t$	= time, sec
$w$	= radial deflection, in.
$x$	= distance along the longitudinal axis of the cylinder, in. (see Fig. 1)
$\theta$	= angle denoting the circumferential location of a point on the cylinder middle surface radius (see Fig. 1)
$\sigma_x, \sigma_\theta, \tau_{x\theta}$	= longitudinal and circumferential direct stresses and shear stress, respectively, psi
$\sigma_b$	= maximum compressive stress due to bending moment
$\sigma_c$	= applied axial stress, positive for compression, $[(M/\pi R^2 h)]$ , psi
$\bar{\sigma}_c$	= theoretical compressive buckling stress for a long cylinder $\{E/[3(1 - \nu^2)]^{1/2}(h/R)\}$ , psi
$\lambda$	= axial wavelength parameter $(m\pi R/L)$
$\Phi$	= wavelength parameter $\lambda/S^{1/2}$
$\gamma$	= specific weight of shell material, lb/in. <sup>3</sup>
$\rho$	= density of shell material $(\gamma/g, \text{lb-sec}^2/\text{in.}^4)$
$\nu$	= Poisson's ratio of cylinder material
$\nabla^4$	= operator $(\partial^4/\partial x^4) + 2(\partial^4/R^2\partial\theta^2\partial x^2) + (\partial^4/R^4\partial\theta^4)$
$\nabla^{-4}$	= inverse operator defined by $[\nabla^{-4}(\nabla^4 f) = f]$
$\omega$	= circular frequency $(2\pi f)$ , rad/sec
$\bar{\Omega}$	= frequency parameter $[12(1 - \nu^2)\rho R^4\omega^2/Eh^2]$

## Introduction

FOR many years, problems of the free vibrations of unloaded or symmetrically loaded cylindrical shells have interested investigators.<sup>1-7</sup> The problem of the free vibra-

Presented at the AIAA Fifth Annual Structures and Materials Conference, Palm Springs, Calif., April 1-3, 1964 (no preprint number; published in bound volume of preprints of the meeting); revision received September 3, 1964. This investigation was performed at the Aerospace Corporation under contract No. AF04(695)-169. The author wishes to thank Greg Johnson for programming the analysis and Anthony DiGiacomo for his help in performing the experimental investigation.

\* Assistant Professor of Civil Engineering. Member AIAA.

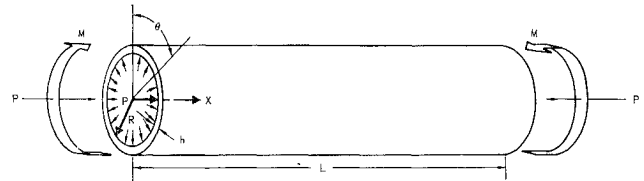


Fig. 1 Notation for problem under consideration.

tions of cylindrical shells subjected to asymmetric loads has remained untouched, however. The particular asymmetric loading of a bending moment applied at the boundaries of a cylindrical shell poses an interesting question. Since a compressive load on a cylindrical shell causes a decrease in frequency, and conversely a tensile load causes an increase in frequency, what happens to the frequency spectrum of a cylindrical shell subjected to a bending moment where half the cylinder is under compression and the other half is under tension? The present investigation attempts to answer this question.

In this paper, the vibrations of a cylindrical shell subjected to a bending moment was investigated by linear theory. The effect of hydrostatic pressure acting in conjunction with the bending moment was also considered. Batdorf's variation of the Donnell equation was modified for the free vibration problem and the Galerkin method used to obtain the frequency determinant. An experimental investigation was also performed to check the analytical results.

## Theory

The Batdorf modification of Donnell's small deflection equation<sup>8</sup> for determining the buckling loads of circular cylinders may be written as

$$Q(w) = D\nabla^4 w + \left(\frac{Eh}{R^2}\right)\nabla^{-4}\left(\frac{\partial^4 w}{\partial x^4}\right) + h\left(\sigma_x \frac{\partial^2 w}{\partial x^2} + \sigma_\theta \frac{1}{R^2} \frac{\partial^2 w}{\partial \theta^2} + 2\tau_{x\theta} \frac{1}{R} \frac{\partial w^2}{\partial w \partial \theta}\right) - q = 0 \quad (1)$$

This equation can be applied to vibration problems of preloaded cylindrical shells if circumferential and longitudinal inertia forces are neglected and the radial surface loading  $q$  is replaced by the radial inertia force

$$-\rho h(\partial^2 w / \partial t^2)$$

We shall consider the free vibrations of a cylinder under combined bending, axial load and external lateral pressure for which the stresses in the shell are given by

$$\sigma_x = \sigma_c + \sigma_b \cos \theta \quad (2)$$

$$\tau_{x\theta} = 0 \quad \sigma_\theta = pR/h$$

where  $\sigma_c = P/2\pi R h$  and  $\sigma_b = M/\pi R^2 h$ .

<sup>a</sup> Values did not converge.

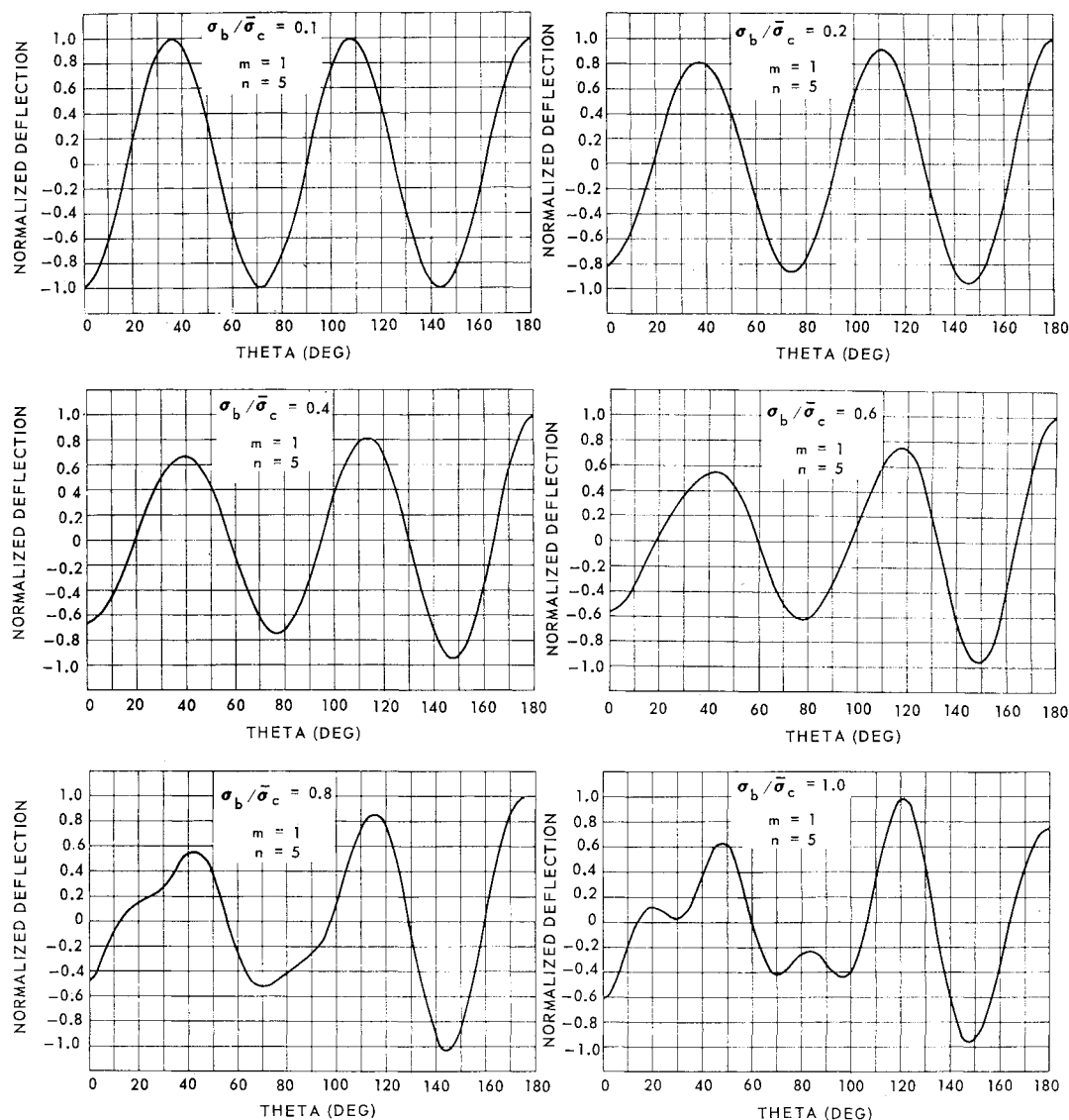


Fig. 3a

Fig. 3 Variation of modal shape with increasing bending moment (Fig. 3b on opposite page).

is the bending moment at which the cylinder buckles and is in good agreement with the results of Ref. 10.

The first problem that arose in the analysis was the identification of modes and frequencies. The mode shapes and frequencies of an unloaded cylinder or a cylinder subjected to uniform axial load or lateral pressure can be identified by an integer corresponding to the number of circumferential waves. For increasing values of  $\sigma_b/\sigma_c$ , the circumferential modal shape (see Fig. 3) became very irregular, and the number of circumferential waves did not have any real meaning. It was found, however, by taking very closely spaced values of  $\sigma_b/\sigma_c$  that one could plot smooth frequency curves from  $\sigma_b/\sigma_c$  equal to zero up to the theoretical buckling value of unity. The value of  $n$  for a given curve in Fig. 2 is the value obtained when  $\sigma_b/\sigma_c$  is equal to zero.

The analytical results plotted in Fig. 2 indicate that as the bending moment becomes larger some of the frequencies increase, whereas others decrease. For example, modes, such as  $m$  equal to 1 and  $n$  equal to 6–9 show a decrease in frequency with bending moment while modes, such as  $m$  equal to 1,  $n$  equal to 5,  $m$  equal to 2, and  $n$  equal to 9 and 12, show an increase in frequency with bending moment. A plot of two modal shapes, one which gives an increase of frequency with bending moment and one which gives a decrease, is shown in Fig. 3. Since the modal shape is symmetrical

about the vertical axis of the cross section, only half the deflection shape is shown in Fig. 3. The angle  $0^\circ$  denotes the point of maximum compressive stress, and  $90^\circ$  the point of zero bending stress. Figure 3a, for  $m$  equal to 1 and  $n$  equal to 5, shows the variation of mode shape when the frequency increases with bending moment. The mode shapes show an increasing maximum deflection on the tension side of the cylinder ( $\theta > 90^\circ$ ) with increasing bending moment. For the case  $m$  equal to 1 and  $n$  equal to 6 shown in Fig. 3b, the frequency increases until  $\sigma_b/\sigma_c$  reaches 0.53 (see Fig. 2) and then decreases with increasing moment until buckling occurs. The mode shapes in Fig. 3b indicate increasing maximum deflection initially on the tension side as the frequency increases and then on the compression side as frequency decreases. We may thus suspect that frequency curves that increase with bending moment correspond to maximum deflection on the tension side and curves that decrease with bending moment correspond to maximum deflection on the compression side.

In addition to vibrations symmetrical about the top of the shell, antisymmetric vibrations were also investigated, with the radial deflection assumed to be of the form

$$w = \sin \frac{m\pi x}{l} \sin \omega t \sum_{n=1}^{\infty} b_n \sin n\theta \quad (6)$$

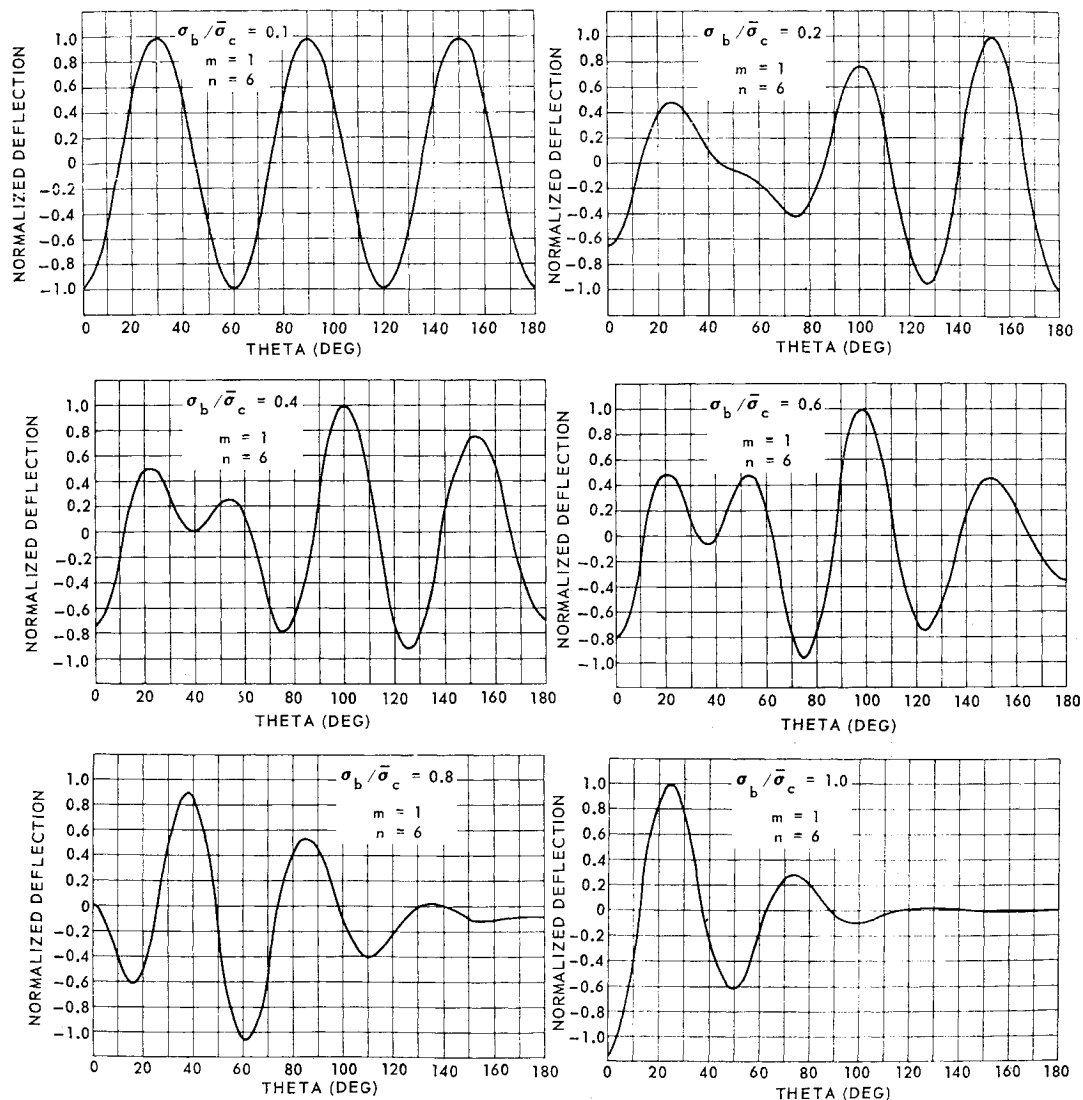


Fig. 3b (Fig. 3a on opposite page.)

The computed frequencies for antisymmetric vibrations were identical with those obtained by using Eq. (3). This result is similar to that obtained by Flügge<sup>9</sup> for the problem of buckling of a cylinder subjected to a bending moment.

### Experimental Investigation

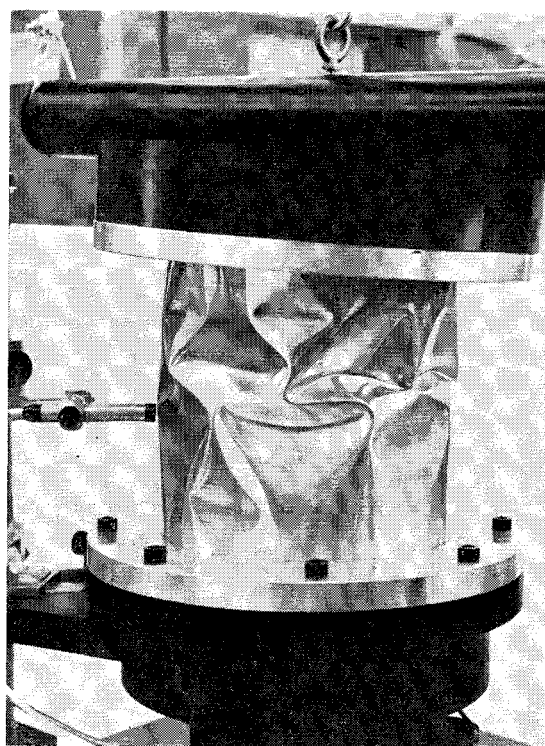
The cylinder used in the experimental investigation had the dimensions and material properties of that of the analytical investigation. It was made of 0.016-in. 6061 aluminum sheet in the T6 condition to insure elastic action and to fit within the load capacity of the test rig. The specimen was first spun on a mandrel, its seam was then butt welded, and finally the cylinder was again spun to insure circularity of the cross section. The cylinder was clamped in grooved aluminum end plates filled with cerrobend, a low melting point alloy. External moment was applied to the loading bar by dead weight acting through cables (see Fig. 4a). The loading bar and upper end caps were counterbalanced to eliminate any axial dead weight loading. The loads applied at the ends of the loading bar were equal and opposite so that a pure bending moment was applied to the cylinder. External pressure was applied to the cylindrical shell by using a pump to evaluate the internal air space. The pressure was measured by a monometer.

Shell breathing mode vibrations were excited by an electromagnet. A condenser microphone, which has a flat response characteristic from 20 to 10,000 cps, was used to measure the

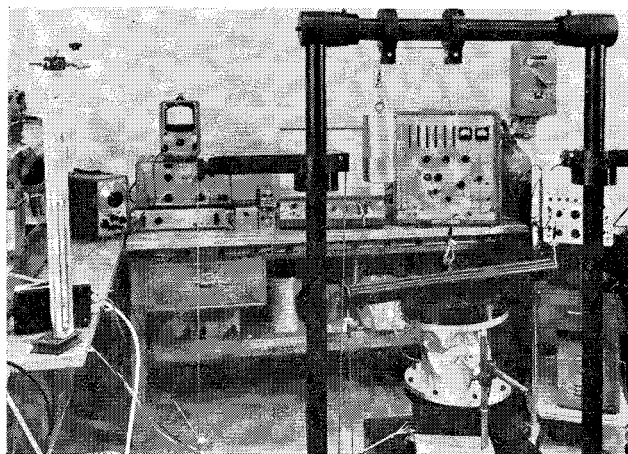
response of the cylinder. The microphone was placed on a track that could be moved along the length of the cylinder and rotated around the cylinder (see Fig. 4b). It was necessary to rotate the microphone since the nodal pattern stayed fixed with respect to the electromagnet.

**Table 2** Tabulation of experimental frequency spectra (cps) as a function of a bending moment parameter ( $\sigma_b/\bar{\sigma}_c$ )

$\sigma_b/\bar{\sigma}_c$	0	0.106	0.168	0.232	0.293	0.355
$n$	$m = 1$					
4	1471	...	...	1509	1441	1435
5	1134	1131	1127	1126	...	1112
6	895	...	893	897	883	878
7	782	761	752	748	734	730
8	747	711	703	692	662	634
9	805	...	803	807	800	...
10	1081	1079	...	1076	...	1071
12	1292	1290	1286	1281	1277	1294
$N$	$m = 2$					
6	1988	2009	1992	1977	1953	1926
7	1655	1663	1675	1646	1631	1637
8	1459	1447	1541	1525	1511	1374
9	1361	...	1441	1415	...	...
13	1833	...	1868	...	...	...



a)



b)

Fig. 4 Test setup.

The test procedure consisted of first applying the desired external pressure and bending moment to the cylindrical shell. The frequency of the current supplied to the electromagnet was varied by means of an oscillator until a resonant frequency was reached. This frequency was accurately measured by a counter connected in parallel to the microphone. The microphone was then moved first in the axial and then in the circumferential direction around the cylinder. The output of the microphone was rectified and recorded on the  $y$  axis of a  $x$ - $y$  plotter. The position of the microphone was measured by means of a balance circuit with an output voltage proportional to its movement and was recorded on the  $x$  axis of the  $x$ - $y$  plotter. A typical record appears in Fig. 5. The minimum points appearing in this figure are node points, since the microphone voltage output is approximately proportional to radial displacement. The applied moment was increased in steps and the frequency spectrum obtained until buckling occurred. The test cylinder in the buckled state is shown in Fig. 4.

The experimental results for the frequency spectrum of the test cylinder under a bending moment and a 2-psi external

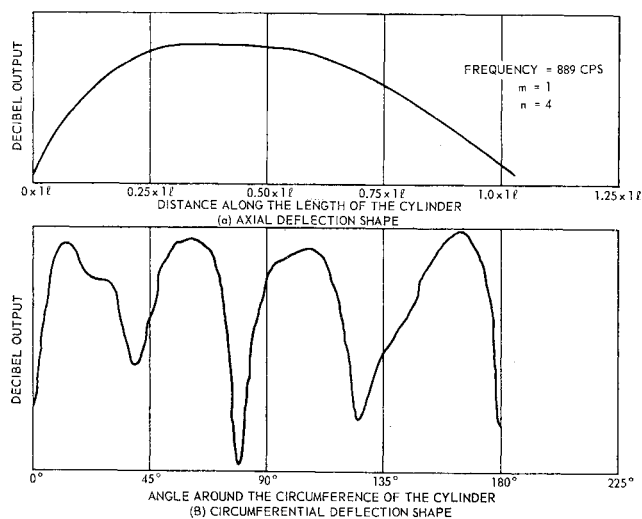


Fig. 5 A typical mode shape record.

pressure appear in Table 2. These results are also plotted in Fig. 2. The experimental results in all cases fall above the analytical curves. This is to be expected since the analysis was done for cylinders with simply supported ends, whereas in the experiment, the specimen ends are somewhere between clamped and simply supported. The experimental results, however, qualitatively check the analysis. For  $m$  equal to 1,  $n$  equal to 6-9, and  $m$  equal to 2,  $n$  equal to 8, the experimental data show a decrease of frequency with bending moment, whereas for  $m$  equal to 2,  $n$  equal to 9, the data indicate an increase of frequency with bending moment as predicted by the analysis.

No experimental results were obtained beyond a  $\sigma_b/\sigma_c$  equal to 0.355, since buckling occurred at a value of  $\sigma_b/\sigma_c$  equal to 0.43. This prevented a check of the large increases and decreases at frequencies occurring beyond this point. A logical extension of this work would be to investigate the combined effect of internal pressure and bending moment, since the buckling value of a test cylinder under this loading would be very close to that predicted by small deflection theory (see Ref. 10), and experimental frequencies could then be obtained up to this point.

## References

- 1 Arnold, R. N. and Warburton, G. B., "Flexural vibrations of the walls of thin cylindrical shells having freely supported ends," *Proc. Roy. Soc. London A* **197**, 238-256 (1949).
- 2 Arnold, R. N. and Warburton, G. B., "The flexural vibrations of thin cylinders," *Proc. Inst. Mech. Engrs.* **167**, 62-74 (1953).
- 3 Weingarten, V. I., "Experimental investigation of the free vibrations of multi-layered cylindrical shells," *Exptl. Mech.* **4**, 200-206 (July 1964).
- 4 Weingarten, V. I., "On the free vibration of thin cylindrical shells," *AIAA J.* **2**, 717-722 (1964).
- 5 Federhofer, K., "Über die Eigenschwingungen der Axial gedrückten kreiszylinderschale," *Sitzungsber. Akad. Wiss. Wien*, **145** (1936).
- 6 Fung, Y. C., Sechler, E. E., and Kaplan, A., "On the vibration of thin cylindrical shells under internal pressure," *J. Aeronaut. Sci.* **24**, 650-660 (1957).
- 7 Koval, L. R. and Cranch, E. T., "On the free vibrations of a thin-walled circular cylindrical shell subjected to an initial static torque," *Proceedings of the Fourth U.S. National Congress of Applied Mechanics* (American Society of Mechanical Engineers, New York, 1962), pp. 107-117.
- 8 Batdorf, S. B., "A simplified method of elastic-stability analysis for thin cylindrical shells, II—Modified equilibrium equation," *NACA TN* 1342 (June 1947).
- 9 Flügge, W., "Die Stabilität der Kreiszylinderschale," *Ing.-Arch.* **3**, 463-506 (1932).
- 10 Weingarten, V. I., "Effects of internal pressure on the buckling of circular-cylindrical shells under bending," *J. Aerospace Sci.* **29**, 804-808 (1962).